Available online at www.sciencedirect.com
SCIENCE DIRECT®
Journal of Catalysis 222 (2004) 419–428
JOURNAL OF CATALYSIS
www.elsevier.com/locate/jcat

# High-resolution electron microscopic, spectroscopic, and catalytic studies of intentionally sulfided $Pt/ZrO_2–SO_4$ catalysts

Marie-Dominique Appay,[a] Jean-Marie Manoli,[a] Claude Potvin,[a] Martin Muhler,[b,1] Ute Wild,[b] Olga Pozdnyakova,[c] and Zoltán Paál [c,*]

[a] *Laboratoire de Reactivité de Surface, URA 1106, Casier 178, Université P. et M. Cuire, F-75252 Paris Cedex 05, France*
[b] *Fritz-Haber-Institut der Max-Planck-Gesellschaft, Faradayweg 4-6, Berlin, D-14195 Germany*
[c] *Institute of Isotope and Surface Chemistry, CRC, Hungarian Academy of Sciences, PO Box 77, Budapest, H-1525 Hungary*

Received 10 July 2003; revised 4 November 2003; accepted 25 November 2003

**Abstract**

Pt (3 wt%)/sulfated zirconia (Pt/SZ) was treated with $H_2S/H_2$ (10% v/v mixture) in the "fresh" (dried) as well as in the "used" state (after calcination and use in an autoclave run under 20 bar $H_2$ and 300 Torr *n*-hexane). Morphological and structural changes as well as the chemical state of sulfur were studied by X-ray diffraction (XRD), X-ray photoelectron spectroscopy (XPS), high-resolution transmission electron microscopy (HRTEM). XPS detected sulfate (BE ∼ 169.5 eV) as the only chemical form of S in the unsulfided catalysts. A sulfide S $2p$ component (BE ∼ 162.5 eV) appeared in the S $2p$ region after sulfidation of both samples. Its amount correlated with the Pt content. Almost all "sulfide" components disappeared from the X-ray photoelectron spectra quasi in situ hydrogen treatment. Ion scattering spectroscopy (ISS) uncovered partly "embedded" Pt in sulfided catalysts and increased the sulfur signal. The $H_2S$ treatment almost completely removed surface carbon impurities. Simulation of the Pt $4f$ peaks by artificial composite spectra of metallic Pt ($Pt^0$), $PtO_{ads}$, and PtS showed that Pt was present as a mixture of $Pt^0$ in close interaction with support oxygens (and/or with an adsorbed O overlayer) and PtS after sulfidation. Using HRTEM several small flat $Pt^0$ particles were detected in unsulfided catalysts. After sulfidation distinct flat $Pt^0$ and PtS particles coexisted. Sulfided catalysts were inactive in benzene and cyclohexene hydrogenation but hydrogen treatment at 573 K reactivated the catalyst for the latter reaction. Thus, the platinum surface accommodated some deactivating chemisorbed sulfur; more S did not, however, form, a compact surface overlayer but appeared as a crystalline PtS phase with discernible lattice distances. Separate PtS particles seen by HRTEM were produced either by total sulfidation of small $Pt^0$ particles or by migration of surface PtS entities from larger Pt crystallites to the support.


*Keywords:* Pt/sulfated zirconia; Sulfur poisoning; Platinum sulfide; HRTEM; XPS; XRD; ISS; Cyclohexene hydrogenation; Benzene hydrogenation; Metal and acid sites

## 1. Introduction

Sulfated zirconia (SZ) catalysts represent a family of highly acidic catalysts exhibiting high selectivity in alkane isomerization [1–3]. Their high activity is short-lived but addition of certain elements, e.g., Fe + Mn [4] or Pt [1–7], may hinder the activity loss. Catalyst activation requires calcination in air at 800–900 K. SZ catalysts are active in the presence of hydrogen only [5–7], with isomerization selectivities up to 100% in the range 400–600 K [6,8].

Active Pt/sulfated zirconia (Pt/SZ) catalysts contain most probably acid sites in close vicinity to Pt sites, both interacting in dissociating hydrogen and transferring hydride ions to the carbenium-type intermediates of isomerization [9,10]. There are counterclaims, however, as for the state of Pt. It was claimed on the basis of X-ray photoelectron spectroscopy (XPS) and the binding energy (BE) shift of the Pt $4f$ peak that a fraction of Pt in the working catalyst must be in the sulfided state [11,12]. The role of differential electrostatic charge in the BE shift has also been pointed out [13]. This is caused partly by the presence of insulating overlayers (oxide and/or sulfide) covering the metallic Pt core [3,12,14,15]. Arguments for this scenario were obtained by X-ray diffraction (XRD), XPS [16], and extended X-ray absorption fine structure (EXAFS) [12,17], as well as

* Corresponding author.
*E-mail address:* paal@iserv.iki.kfki.hu (Z. Paál).
[1] Present address: Lehrstuhl für Technische Chemie, Ruhr-Universität Bochum, D-44780, Bochum, Germany.

0021-9517/$ – see front matter 
doi:10.1016/j.jcat.2003.11.014

by the dramatic drop in hydrogen chemisorption ability of reduced Pt/SZ catalyst [14]. Counterclaims were made with respect to the oxidic or sulfidic character of this overlayer. Sulfur arising from reduction of sulfate groups was reported to poison the platinum function [19]. The pronounced hydrogen spillover and isomerization by the close cooperation of acid–metal sites [7,18,19] would, however, require maintaining some $H_2$ chemisorption ability, on $Pt^0$ centers. A fraction of sulfate groups seem to undergo reduction to $S^{4+}$ by an "oxidative" start of alkane reaction [20] and can be reduced further to $S^{2-}$. A sulfide peak appeared in the S $2p$ core-level spectra of a Pt/SZ catalyst after treatment of it with $H_2$ in the preparation chamber of the spectrometer, most pronounced on a calcined Pt/SZ after several runs of *n*-hexane reactions but still far from complete deactivation [21].

The present article attempts to approach the problem from the other route. We intentionally sulfided samples containing 3% Pt on sulfated $ZrO_2$. In this way a surface was created where there was certainly some sulfide present. Pt/SZ catalysts before calcination [22], as well as a calcined sample used in *n*-hexane isomerization reactions [23], were sulfided. Similar treatments created Pt sulfide entities on the surface of various Pt catalysts [24,25]. Thus, the amount of this added sulfide and its stability under a reductive treatment could be studied. Results of electron spectroscopy (XPS) and high-resolution transmission electron microscopy (HRTEM) are reported. Lattice interfringe measurements were used to identify small Pt and PtS particles and the (sulfated) zirconia "support." Transmission electron microscopy allowed us to observe the entities obtained and could confirm and even extend the conclusions drawn on the basis of electron and ion spectroscopy, giving rise to new suggestions. By comparison of these results with those of catalytic tests, a completely new approach to describing the state of partially sulfided Pt/SZ catalysts is proposed.

## 2. Experimental

Samples containing ca. 3% Pt were prepared as described earlier [22] and used without calcination (code: "fresh"). Another sample (code: "used") was calcined at 900 K and then brought into contact with a mixture of *n*-hexane (nH) and $H_2$ (1:10) in a flow reactor at 1 bar at 373 K for several hours followed by a run of hours in a nonstirred autoclave at 20 bar $H_2$ and the same nH pressure [23]. Fractions of both catalysts were treated isothermally in a flow system at 673 K, as described earlier [24], with a mixture of 10% $H_2S$ plus 90% $H_2$ (codes: "fresh/S" and "used/S"). The samples were stored in air between different tests.

All sulfided Pt/SZ samples were investigated by HRTEM, and compared with their unsulfided precursors. A few milligrams of powder samples was ultrasonically dispersed in absolute ethanol. A drop of this suspension was deposited to evaporation on a metallic grid covered by a holey amorphous carbon film. The samples were observed in a JEOL 100CX II electron microscope. Raw HRTEM images with magnifications of 330,000 and 470,000 were recorded on classic $6 \times 9$-cm negatives (about six high-resolution micrographs were studied for each sample). These were numerized using a ThetaScan Umax scanner at a resolution of 2000 ppi. The acquired images were processed (magnified and contrasted) with Photoshop software. The interfringe distances could be measured directly on these magnified micrographs. The measurements were confirmed by Fourier transform images obtained using a local software on numerized parts of the negatives. The lattice distances were compared with JCPDS files (or with interfringes calculated from JCPDS files) of the species possibly present in the chemical system considered.

Two sulfided samples ("fresh/S," "used/S") were studied by X-ray diffraction (XRD), as well as by XPS and ion scattering spectroscopy (ISS), as described earlier [21–23]. A $H_2$ treatment was also possible in the preparation chamber of the electron spectrometer; representing a quasi in situ reduction in a sense that no air exposure took place between hydrogenation and subsequent XPS measurement. This was done at 653 K. No XPS study was possible *during* contact of the sample with $H_2$. The code "$+H_2$" was added to the code of these samples. Samples after ISS are denoted by adding "+ISS" to their code.

### 2.1. Catalytic tests

Hydrogenation of benzene and cyclohexene was used to test catalytic propensities. Three milligrams of catalyst was loaded into a pulse reactor and pulses of 0.5 µl were introduced into a hydrogen flow of 60 mL $min^{-1}$ between 325 and 383 K, in the "as received" state as well as after being heated in $H_2$ flow up to 573 K.

## 3. Results

### 3.1. X-ray diffraction

The X-ray diffraction pattern of the "fresh" catalyst showed rather poorly crystallized $ZrO_2$, together with well-developed Pt lines indicating a Pt crystallite size of ca. 10 nm [22]. Heating up to 673 K during sulfidation represented obviously a sort of "low-temperature calcination" and improved the crystallinity of zirconia, forming its tetragonal modification. The "used" catalyst appeared as a tetragonal zirconia but the Pt lines were less pronounced, as reported earlier [22]. The Pt lines showed hardly any changes on sulfidation and no lines attributable to Pt sulfide phase(s) appeared, in agreement with the low sensitivity of XRD to components present in small amounts (Fig. 1). The situation was different for $Pt/MoO_x/Al_2O_3$, where the appearance of PtS crystallites in electron microscopy—with well-identifiable electron diffraction—was accompanied by a minor XRD shoulder of PtS phase [26].

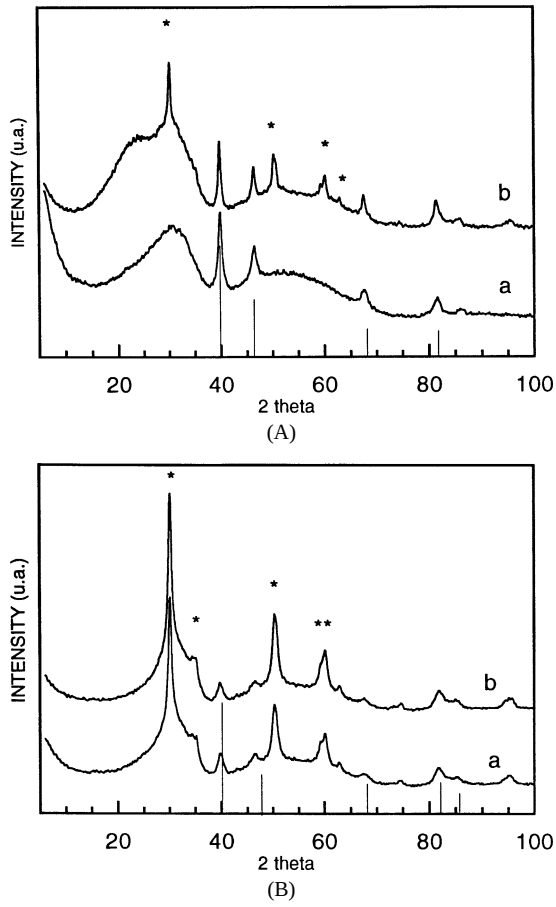


Fig. 1. X-ray diffraction patterns of unsulfided (curves a) and sulfided (curves b) catalysts. Asterisks denote the diffraction lines of tetragonal $ZrO_2$ (JPCD 17-0923), and vertical lines, those of Pt metal (JPCD 4-0802). PtS could not be detected. The crystallinity of zirconia was higher in the case of "used" catalyst, but the intensity of Pt was much lower. (A) "Fresh" catalysts; (B) "Used" catalysts.

### 3.2. High resolution transmission electron microscopy

#### 3.2.1. Unsulfided samples

The current study revealed two kinds of metallic Pt particles. Some particles were large and dense [e.g., $\sim 50 \times 140$ nm, lattice plane: (111)]. This result agrees well with Pt reflections observed by XRD. These particles displayed a characteristic half-moon shape, as shown earlier [22]. The other type of particle was thinner and smaller. It appeared flat and rounded (diameter: $\sim 5$ nm) or elongated ($\sim 10 \times 5$ nm). Their size is in agreement with measurements reported by Smith et al. [27] and Chang et al. [28] on $Pt/A_2O_3$, but somewhat larger than those reported by van Gestel et al. on Pt/SZ [29]. In the latter study the lower Pt loading (0.025 to 0.8 mass%) could explain the smaller Pt particles ($\sim 1$ nm). The lattice fringe measurement has led us to identify several crystallographic planes—(110), (111) and (020)—in fcc metallic Pt. Table 1 also contains results for larger particles described in earlier articles [22,23] and subjected to the present image processing. Detection of Pt(110) forbidden reflections has already been reported by Roberts and Gorte [30] and noted as $\frac{1}{2}(-220)$ reflection in flat $Pt^0$ particles. In the same way, on sulfated zirconia, interfringes with a periodicity of 0.277 nm and corresponding to these forbidden reflections were detected in flat Pt particles. These forbidden reflections could be due to the "lack of complete Pt unit cell" [30]. These small $Pt^0$ particles do not produce XRD reflections.

Table 1
Particle size and interfringe measurements of Pt particles in unsulfided samples from high-resolution transmission electron micrographs

| Sample | Particle size (nm) | Lattice interfringe, $d$ (nm) | | Identification | Comment |
|---|---|---|---|---|---|
| | | Measured | Literature value | | |
| Fresh | $15 \times 5$ | 0.228 | 0.227[a] | $Pt^0(111)$ | Ref. [22] |
| | 4.5 | 0.275 | 0.277[a,b] | $Pt^0(110)$ | |
| | $4 \times 2$ | 0.278 | 0.277[a,b] | $Pt^0(110)$ | |
| Used | $12 \times 5$ | 0.195 | 0.196[a] | $Pt^0(020)$ | Ref. [23] |
| | $8.5 \times 6$ | 0.225 | 0.227[a] | $Pt^0(111)$ | |
| | $8.5 \times 5.5$ | 0.191 | 0.196[a] | $Pt^0(020)$ | |
| | $4 \times 3$ | 0.226 | 0.227[a] | $Pt^0(111)$ | |
| | $6 \times 4$ | 0.228 | 0.227[a] | $Pt^0(111)$ | |

[a] Referred to and calculated from JCPDS 4-802.
[b] As observed by Roberts and Gorte [30].

The zirconia particles were sintered, as opposed to other preparation processes [31] where $ZrO_2$ remained as small individual particles. Tetragonal $ZrO_2$ is the main crystallographic species (as detected by XRD). Nevertheless, since the support appeared nonhomogeneous and formed collapsed crystal particles, its heating was probably not uniform. This is why remaining monoclinic domains exhibited planes of (111) (−210) could be detected at the zirconia surface. The coexistence of monoclinic and tetragonal $ZrO_2$ and their interconversion at different heating temperatures were reported by Vera et al. [32]. Local warming by the electron beam might generate monoclinic zirconia as a microscopic surface species undetectable by XRD (Fig. 1).

Calcination caused no dramatic Pt particle size growth [22]. The electron micrographs of the "used" catalyst—subjected to *n*-hexane reactions—revealed no changes in Pt particle sizes published earlier [23]. Thus, the "using" process did not appear at the ultrastructural level, i.e., regarding particle size and distribution or chemical transformations.

#### 3.2.2. Sulfided samples

Analysis of electron micrographs of the sulfided "fresh" sample revealed two kinds of thin particles: metallic $Pt^0$ (110) and PtS (101). Both are shown in Fig. 2, together with some monoclinic $ZrO_2$. The PtS particles could be flat and elongated ($7.5 \times 5$ nm) or rounded ($\sim 7$ nm).

The "used" sample after sulfidation showed the same type of PtS particles [planes (101) and (100)] (Table 2). On the right-hand side of Fig. 3 a rounded particle exhibits two sets of fringes belonging to PtS and Pt crystallographic lattices. The fringes of PtS are connected to those of Pt and con-

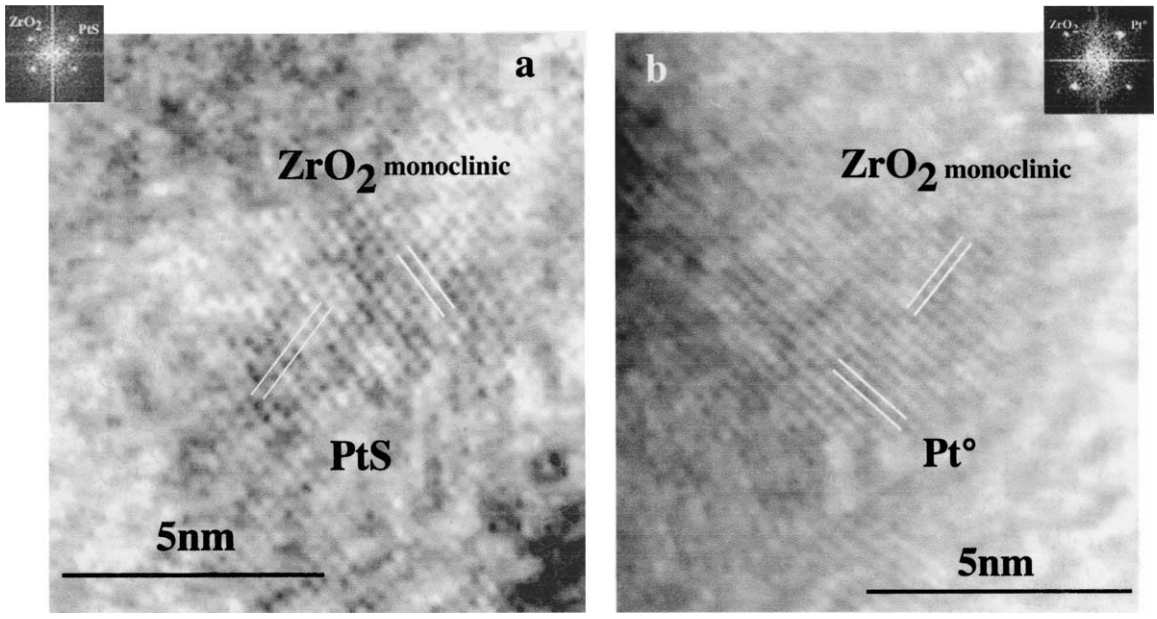


Fig. 2. High-resolution transmission electron micrographs of Pt and PtS particles detected at the surface of the "fresh" sulfided Pt/zirconia sample. (a) Flat elongated PtS (101) of 9.3 × 4.4 nm resting on monoclinic $ZrO_2$(111) [JCPDS 37-1484]. (b) Flat rounded metallic Pt (110) of 4.2 nm diameter lying on monoclinic $ZrO_2$ (−210) [JCPDS 37-1484]. The insets show the Fourier transform patterns of the different particles.

Table 2
Particle size and interfringe measurements of Pt particles in sulfided samples from high-resolution transmission electron micrographs

| Sample | Particle size (nm) | Lattice interfringe, *d* (nm) | | Identification | Comment |
|---|---|---|---|---|---|
| | | Measured | Literature value | | |
| Fresh/S | 4.4 × 3 | 0.275 | 0.277[a,b] | $Pt^0$(110) | |
| | 3.6 × 3.8 | 0.302 | 0.302[c] | PtS(101) | |
| | 9.3 × 4.4 | 0.303 | 0.302[c] | PtS(101) | Fig. 2a |
| | 4.2 | 0.275 | 0.277[a,b] | $Pt^0$(110) | Fig. 2b |
| Used | 11.2 × 5.1 | 0.302 | 0.302[c] | PtS (101) | Fig. 3 |
| | 11 | 0.271 | 0.277[a,b] | $Pt^0$(110) | Figs. 3, 4[d] |
| | 6 × 5 | 0.300 | 0.302[c] | PtS(101) | Figs. 3, 4[d] |
| | 5 | 0.302 | 0.302[c] | PtS(101) | |
| | 4.5 | 0.303 | 0.302[c] | PtS(101) | |
| | ∼4 | 0.348 | 0.347[c] | PtS(100) | |

[a] Calculated from JCPDS 4-802.
[b] As observed by Roberts and Gorte [30].
[c] Referred to JCPDS 18-972.
[d] Mixed particle (Figs. 3 and 4).

trasted at the same level, that is, stayed in the same plane. Moreover, the PtS part exhibits crystallographic defects suggesting that the PtS network is developing (Fig. 4). Figs. 2 and 3 demonstrate that metallic Pt remains distributed as thin particles throughout the support, despite $ZrO_2$ aggregation, and that sulfidation can develop progressively in situ from thin metallic Pt.

Aggregation of zirconia was observed in all samples and this could induce embedding of some metallic Pt particles [22,29], as shown also by ISS (see below). In addition, seems that Pt particles did not grow oriented on $ZrO_2$ crystals, since three different interfringe planes have been measured for $Pt^0$.

### 3.3. X-ray photoelectron spectroscopy

Table 3 summarizes the surface compositions of the samples studied after various stages of their life. The Zr/O ratio increased on sulfidation due to removal of water and/or hydroxyl overlayer after heat treatments: during calcination at 900 K ("fresh" vs "used" sample), and even during the moderate heating in sulfidation. Hydrogen treatment in the spectrometer resulted in segregation of carbon on the surface and in a slight enrichment of Pt and depletion of S (removal of the sulfide component from Pt). The $He^+$ ions of 2 keV used in ISS exerted a mild sputtering effect [24]. They removed almost all surface carbon from the sulfided "fresh" catalyst, whereas the amounts of S and Pt component—lying obviously in positions not visible by XPS [33]—increased slightly more than what was expected based on the concentration change of carbon. The "used" catalyst had a much lower surface Pt concentration (Table 3), due to precalcination before nH reactions. Its sulfidation (involving heat treatment) and reduction caused fewer composition changes than in the case of "fresh" Pt/SZ catalyst.

The O 1*s* line had a peak at ca. 530.5 eV binding energy (BE) corresponding to oxygen in zirconia. Another component at ca. 532 eV [22] may correspond to sulfate [34] or zirconium hydroxide [35]. The abundance of the latter component decreased on sulfidation and increased after subsequent hydrogen treatment. Similar conclusions were drawn from the changes in the Zr 3*d* doublet during various treatments [21,22]. The narrower Zr 3*d* doublet on ISS treatment pointed to a decrease in the ZrOH component. The Zr/O ratio increased during these stages (Table 3). The O 1*s* region of the "used" catalyst showed smaller changes during sulfidation and subsequent reduction. The preceding agrees well

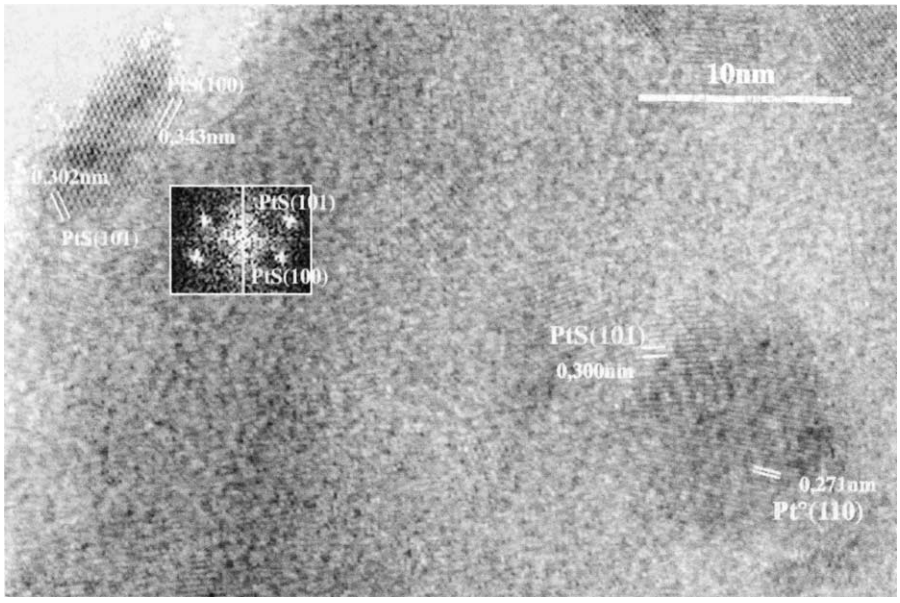


Fig. 3. High-resolution transmission electron micrograph of Pt and PtS particles in the "used" sulfided Pt/zirconia sample. On the left, two sets of fringes have been measured belonging to the PtS crystallographic system. As the angle of 50° between the two sets of fringes is incompatible with the tetragonal lattice, these sets do not belong to the same but rather to two different particles. Inset: Fourier transform pattern of the particle. On the lower right a mixed Pt/PtS has been detected. Two sets of fringes have been measured in the same particle area. Some Pt(110) interfringes are connected to the PtS(101) interfringes.

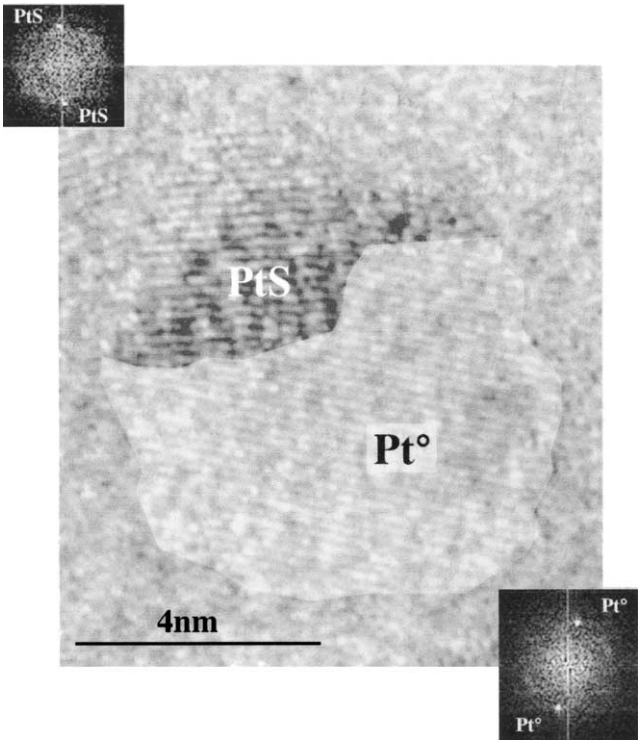


Fig. 4. Higher magnification of the mixed particle shown in Fig. 3. Selected area contrasting using Photoshop software allows enhancement and confirmation of the structure of this complex configuration. Inset: Fourier transform pattern of the particle.

with the coexistence of two crystalline phases of zirconium oxide found by HRTEM, including, the possible presence of a hydroxide component.

Table 3
Surface composition of the samples[a]

| Sample | Composition (%) | | | | | | | | Zr/O ratio |
|---|---|---|---|---|---|---|---|---|---|
| | O | Zr | S | Within S | | Pt | C | Si | |
| | | | | Sulfate | Sulfide | | | | |
| Fresh[b] | 57.4 | 18.2 | 3.3 | 3.3 | – | 2.5 | 12.3 | 5.4 | 0.32 |
| Fresh/S | 66.5 | 23.7 | 4.7 | 3.3 | 1.4 | 1.8 | 0.9 | 2.4 | 0.36 |
| Fresh/S/H | 60.8 | 24.0 | 2.5 | 2.2 | 0.3 | 2.3 | 6.5 | 3.7 | 0.39 |
| Fresh/S/ISS | 64.0 | 26.0 | 3.9 | 2.5 | 1.4 | 2.8 | 0.1 | 3.2 | 0.40 |
| Used[c] | 67.5 | 22.1 | 4.0 | 4.0 | – | 0.4 | 3.0 | 2.9 | 0.32 |
| Used/S | 68.9 | 24.6 | 3.0 | 2.4 | 0.6 | 0.4 | 0.6 | 2.2 | 0.36 |
| Used/S/H | 65.7 | 26.5 | 2.3 | 2.2 | 0.1 | 0.5 | 1.9 | 3.1 | 0.40 |

[a] Based on XPS line intensities of O 1*s*, Zr 3*d*, S 2*p*, Pt 4*f*, C 1*s*, and Si 2*p*. Sample identification, see Experimental.
[b] Ref. [22].
[c] Ref. [23].

Sulfate with a BE maximum at 169.5 eV was the only component in the S 2*p* region of both "fresh" and "used" samples in the "as received" state. As indicated in the literature [11,14,19,21] contact with $H_2$ at 653 K partly reduced this sulfate to $S^{2-}$. This reduction was minor on both "fresh" and "used" samples, but a more pronounced sulfide peak appeared when a Pt/SZ used previously in hexane reactions between 420 and 600 K was treated in the preparation chamber with $H_2$ at 653 K [21]. We can assume a relatively small amount of sulfide in the "normal" state in the period of "quasi-steady" activity of Pt/SZ after regeneration with hydrogen between catalytic runs. The Pt/SZ catalyst showed higher isomerization selectivity versus cracking in this state [21].

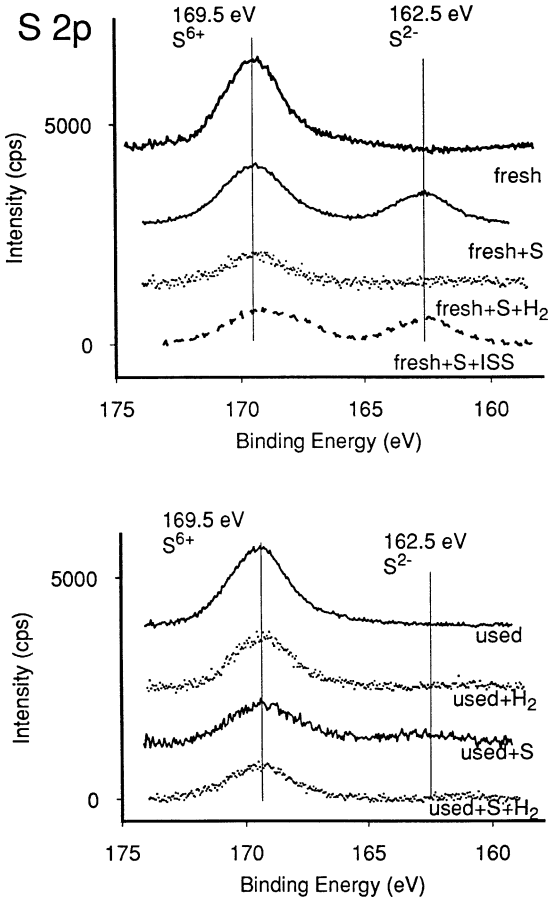


Fig. 5. S $2p$ region of the samples after different treatments. Top: "fresh" catalysts; bottom "used" catalysts.

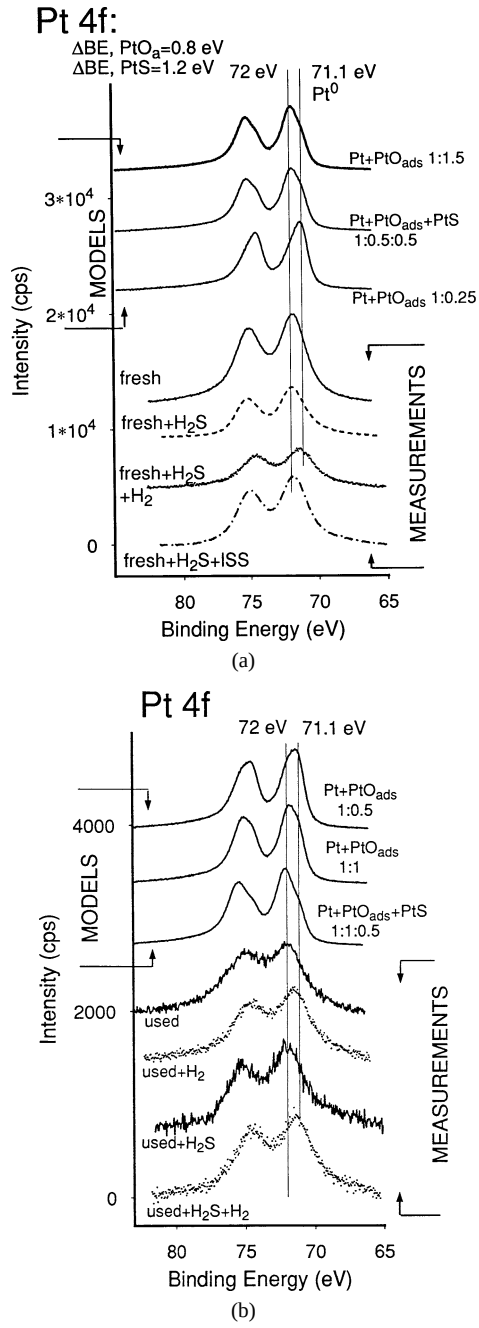


Fig. 6. Pt $4f$ region of samples after different treatments: (a) "fresh" catalysts; (b) "used" catalysts. Calculated model curves of various composition ($Pt + PtO_{ads} + PtS$) have been added to both (see text).

The lower S concentration after treatment with $H_2S$ (Table 3) is concomitant with the increase in Zr percentage and, thus, can be connected to aggregation/recrystallization of zirconia. The appearance of sulfide peaks in the S $2p$ region in both catalysts (Fig. 5) agrees with the presence of the PtS component found by HRTEM. Its amount was much less on the "used" catalyst. Heating in hydrogen up to 650 K removed most of the sulfide component in both cases, leaving the sulfate peak unchanged. The abundance of sulfide increased again after ISS treatment of the sulfided "fresh" catalyst, presumably due to the reductive effect of $He^+$ ion bombardment, as also described for other systems [36].

The Pt $4f$ region for the "fresh" catalyst after the treatments specified above is shown in Fig. 6A, and that for the "used" catalyst, in Fig. 6B. Experimental curves are shown together with results of model calculations. For the latter purpose the Pt $4f$ peak of a purified Pt black catalyst [24] was used. Shifting its BE by 0.8 eV would correspond to the position of Pt containing chemisorbed oxygen [37]. The BE shift for PtS was taken to be 1.2 eV [38,39]. Model spectra corresponding to various mixtures of Pt, $PtO_{ads}$, and PtS were calculated. Mixed spectra resembling the experimental curves were selected. We adjusted the size of the model spectra to the very different Pt intensities of the "fresh" and "used" samples.

Two factors must be considered when the calculated and measured spectra are compared. First, close model compositions often gave rather similar shapes (e.g., for $Pt:PtO_{ads} =$ 1:1 or 1.5:1). Second, the shape of the measured spectra is typical of disperse supported Pt particles, showing line broadening [25,40]. The separation of the Pt $4f_{5/2}$ and Pt $4f_{7/2}$ components is, therefore, poorer than in the model spectra. The BE shift due to particle size effect [41] should

play a minor role with particle sizes of a few nanometers (corresponding to a few hundred Pt atoms, as calculated also from transmission electron micrographs) (Table 2).

The state of Pt in the untreated "fresh" sample may correspond to the mixture of Pt and $PtO_{ads}$, the latter being in excess. In fact, $Pt^0$ particles were detected by HRTEM. After $H_2S$ treatment, the composition was approximated with a mixture of Pt with much less $PtO_{ads}$ plus PtS. Hydrogenation removed the sulfide component from the S $2p$ region (Fig. 6); the model spectrum containing Pt with even less $PtO_{ads}$ was selected to represent this state. ISS brought back the sulfide component and shifted the Pt $4f$ peaks also toward higher BE values. No actual model is given to simulate this state.

The partial "embedding" of Pt into bulk zirconia [22,29] may be the main reason why the intensity of the Pt $4f$ peaks is much lower in the "used" sample. The tentative simulation with model spectra was given as $Pt + PtO_{ads}$ in the untreated sample to which PtS is added after sulfidation. The higher contribution of the "PtO" component in the simulation may originate from an oxidic overlayer [12] or from the interaction of the small and partly embedded Pt particles with support oxygen atoms [42].

The untreated catalysts contain rather large amounts of carbon (Table 3) as an impurity, as also found for other supported catalysts [40,43]. It comprises adventitious carbon accumulated during storage in air, as well as residues from previous reactions in the case of "used" samples [23]. The peak for carbon impurity contained a main component at ca. 284.8 eV and also a smaller shoulder at ca. 289 eV (oxidized carbon, e.g., carboxyl groups). This "oxidized carbon" component may belong partly to carbonaceous residues attached to strongly acidic centers, i.e., "acidic coke" [44]. $H_2S$ treatment removed surface carbon almost completely (Table 3). This effect was more pronounced with the "fresh" sample than with the used catalyst, corresponding to the different origins of carbon; polymerized residues after hexane reaction were more resistant. More carbon was observed after hydrogen treatment: $H_2$ must have mobilized C in positions invisible by XPS, as reported, e.g., for $Pt/SiO_2$ [40]. ISS removed carbon from the outer surface rather efficiently.

### 3.4. Ion scattering spectroscopy

The sulfided "fresh" catalyst sample was studied by the very surface-sensitive but semiquantitative method [45]: ion scattering spectroscopy under quasi-steady-state conditions. The ion scattering spectra showed a rather intense Zr peak together with oxygen of lower intensity (Fig. 7). The carbon region was outside the range studied. The Pt signal increased during subsequent scans, indicating the removal of surface impurities and release of platinum "embedded" under zirconia layers [22,23,29]. The Pt intensities of sulfided and unsulfided samples were close. The sulfur signal was rather weak. Thinning of the layer of powdered samples under the sputtering effect of the $He^+$ ions gave rise to sample holder signal (stainless steel).

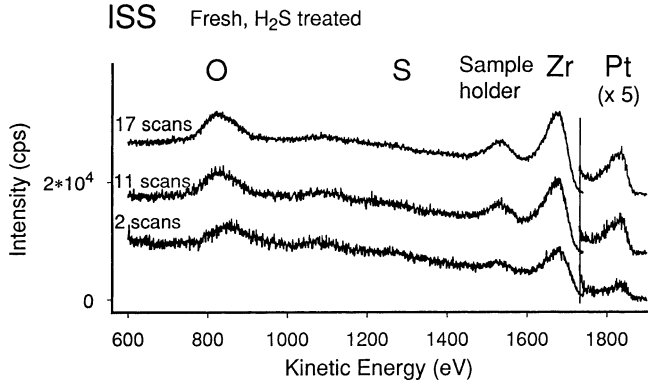


Fig. 7. Ion scattering spectra of sulfided "fresh" Pt/sulfated zirconia catalyst in three different stages of sputtering. The increasing Pt intensity during subsequent scans indicates its uncovering by the sputtering effect of $He^+$ ions. The intensity of the Pt signal was multiplied by a factor of 5 for clarity.

Table 4
Residual activity ($X/X_0$) of various catalysts in hexane test reaction after different pretreatments[a]

| Catalyst | Conversion (%) | | | | | |
|---|---|---|---|---|---|---|
| | Benzene hydrogenation | | | Cyclohexene hydrogenation | | |
| | 343 K | 363 K | 383 K | 343 K | 363 K | 383 K |
| Fresh | 28 | 36 | 43 | 47 | 54 | 62 |
| Fresh/S | 0 | 0 | 0 | 0 | 0 | 0 |
| Fresh/S/H | 0 | 0 | 6 | 10 | 30 | 40 |
| Used | 16 | 34 | 40 | 33 | 41[a] | 45[a] |
| Used/H | 0 | ~1 | ~2 | 0 | 10 | 34[a] |
| Used/S | 0 | 0 | 0 | 0 | 0 | 0 |
| Used/S/H | 0 | 0 | ~3 | 38 | 47 | 55 |

[a] Traces of methylcyclopentane (< 0.3%).

### 3.5. Catalytic tests

Test reactions can be the best method to characterize the catalytic propensities of a surface. Benzene hydrogenation was used to probe the metallic state of Pt/SZ catalysts [19]. Table 4 compares the results obtained in this reaction as well as in the hydrogenation of cyclohexene. The unsulfided catalysts were active in both reactions; the higher Pt content of the "fresh" Pt/SZ was more active. Sulfided catalysts in the "as received" state were, however, inactive in the hydrogenation of both benzene and cyclohexene. Benzene formed traces of cyclohexane after treatment in $H_2$ flow up to 353 K. The same treatment, however, totally re-activated the catalyst in the cyclohexene reaction. Similar $H_2$ treatment of the parent, unsulfided Pt/SZ decreased somewhat the hydrogenation activity in both reactions.

## 4. Discussion

XPS provided information as to the chemical state of Pt/SZ catalysts under reaction conditions. Zirconia containing much sulfate was detected, and, on $H_2$ treatment, some S in the sulfidic state appeared [21,22]. XRD revealed most zirconia in the tetragonal form [22], reported to be necessary to anchor sulfate groups in a catalytically active form [46,47]. The amount of sulfate seemed to have an optimum [48] for the best catalytic activity. At lower $H_2$ pressures, a positive hydrogen order appeared, reaching in most cases a maximum, followed by a negative hydrogen order section [6,7,9,10,22]. There is no agreement in the literature on the reason for the activity decay at higher $H_2$ pressures. One reason may be excess hydrogen promoting the reduction of sulfate, thus decreasing the activity of the metallic sites. Removal of sulfate from 573 K upward caused, indeed, lower overall activity [49]. Similar treatment decreased the rate of *n*-octane hydrocracking isomerization [19]. Hydrogen flow may have also removed surface sulfide, as shown by the activity in benzene hydrogenation [19]. The relative amount of $S^{2-}$ produced by quasi in situ $H_2$ treatment of a calcined Pt/SZ [21] was close to that arising after sulfidation (Fig. 5).

Previous models suggested that Pt would exist in the form of PtO and PtS with a smaller amount of $Pt^0$ [11,12], possibly as a *metallic "core"* covered by oxide and sulfur *overlayers* [13,14]. The present XPS study provides evidence that the state of Pt can be well described as a mixture of $Pt^0$ with oxidized Pt and PtS (Figs. 6a and b). The oxygenated component can be present as a chemisorbed O layer ($\Delta$BE $\sim$ 0.8 eV [37] rather than PtO compound ($\Delta$BE $\sim$ 2.3 eV). $H_2S$ interacts directly with Pt particles, forming PtS, appearing in XPS as $S^{2-}$ and confirmed by EM. Where the amount of Pt is smaller, the intensity of the $S^{2-}$ peak is also lower (Fig. 5). The "balance" between $S^{2-}$ and Pt (Table 3) indicates, however, that some sulfur must be attached to zirconia sites (as shown also by the increasing Zr/O ratios).

HRTEM of sulfided Pt/SZ provides information on an advanced stage of the interaction between Pt and sulfur. This process could transform smaller Pt particles quantitatively into PtS which could be detected as a separate phase by EM (Figs. 2 and 3). Fig. 4 shows a remarkable example of the coexistence of Pt metal and PtS demonstrating this ongoing process. As no big PtS particles could be detected and as no thin PtS fringes could be observed on the coarse Pt particles, the "nascent" PtS phase could detach from their mother Pt particles. They might migrate ("surf") onto zirconia (Fig. 8), because of the better "solid–solid wetting" [50] between PtS and the oxide support. This kind of "surfing" has been proposed as the initial step in detachment of PtO from $Pt^0$ [51]. XPS (Fig. 6) indicates that oxygen is present as adsorbed entities on Pt; thus no separate "PtO" phase [37] is present: no PtO fringers are seen in HRTEM. A similar phenomenon was reported for the mobility of the PtO overlayer migrating on oxidative treatment of metallic Pt to the support [52].

Catalytic tests could decide if the formation of PtS phase and its detachment would leave behind clean or partly sulfided Pt. Sulfidation effectively poisoned benzene hydrogenation (Table 4), requiring three Pt-atom ensembles with (111) symmetry [53]. This catalyst was also inactive in cyclohexene hydrogenation which could also take place on smaller Pt ensembles [54]. High-temperature hydrogen treatment removing most sulfide (Fig. 5) reactivated the sites necessary for this latter reaction, but the overwhelming majority of sites for benzene hydrogenation were still inactive (Table 4). This might be attributed to the presence of "disperse" surface sulfur. The situation is similar to $Pt/Al_2O_3$ containing 1/8 monolayer Ge [55] active in cyclohexene and inactive in benzene hydrogenation. The poisonous species may contain $S^{2-}$ as well as $S^{n+}$. This latter species was a major component on sulfided supported Pt [25]. These "sulfate" entities are independent of the acidic sulfate groups on zirconia and, because their amount is small, they cannot be observed separately. $H_2$ treatment of unsulfided Pt/SZ also caused some deactivation, confirming the possibility of reduction of some sulfate groups [14,19]. The acidic sites exhibited minimal activity, as shown by the formation of almost negligible traces of methylcyclopentane formed from cyclohexene.

XPS, as a macroscopic method averaging information from several billion atoms, would not distinguish (i) Pt with chemisorbed S, (ii) a PtS phase *over* Pt particles, and (iii) separate PtS entities in their vicinity, since the line broadening due to electrostatic charging and particle size effects would cover all these finer effects. HRTEM allowed observation of species iii. EXAFS showed PtS formation and Pt agglomeration on sulfur poisoned $Pt/Al_2O_3$ [28], but separated Pt and PtS particles (Figs. 2 and 3) have not been reported before the present study. Catalytic measurement, in turn, pointed to the presence of type i species.

Interaction with the hydrocarbon reactant could also destroy PtS sites, as found with repeated runs of *n*-hexane reactions on sulfided Pt black, resulting in gradual recovery of the catalytic activity with a concomitant decrease in the sulfided Pt component [24]. The decrease in carbon content after $H_2S$ treatment (Table 3) also indicates a mutual interaction of $H_2S$ and hydrocarbons, even if the latter species form a residual hydrocarbonaceous overlayer, mainly on acidic SZ sites [56]. The hypothetical migration of Pt sulfide contributes to the destruction of surface C layers. This effect is in agreement with the lower coke content of prereduced Pt/SZ catalysts [19]. Further investigation could clarify the interaction(s) between surface carbon and hydrogen sulfide.

## 5. Conclusions

Treating Pt/sulfated zirconia catalysts with a mixture of $H_2S$ and $H_2$ gave rise to sulfide entities, detectable by XPS: as a "sulfide" component in the S $2p$ region and an apparent "PtS component" in the Pt $4f$ region. The latter shows

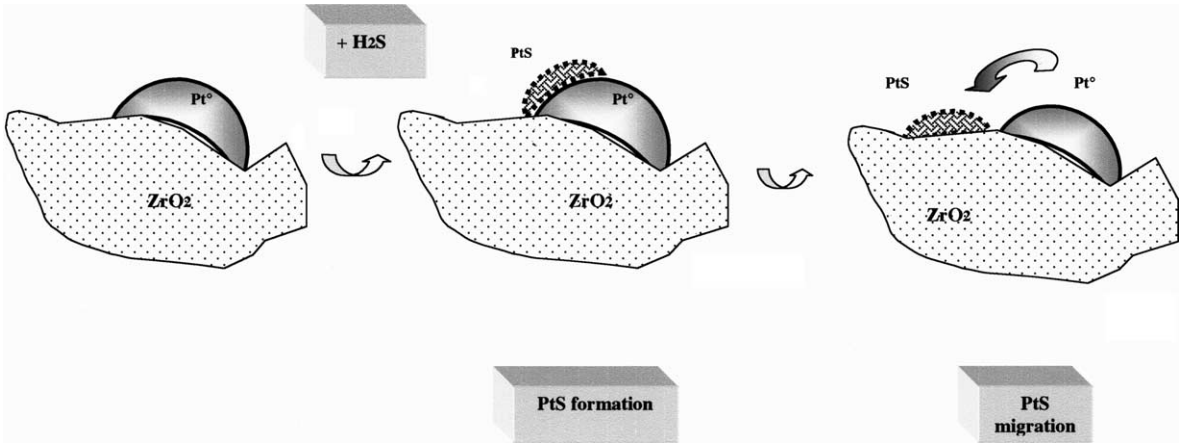


Fig. 8. Scheme of hypothetical PtS formation on coarse $Pt^0$ particles. $H_2S$ induces the formation of flat PtS particles at the surface of coarse Pt crystallite. PtS could then detach from the $Pt^0$ surface and migrate ("surf") onto the zirconia support.

incomplete sulfidation of Pt, $Pt^0$ and "PtO" components always being present.

Sulfidation must have started as forming surface ("chemisorbed") sulfur. No PtS component was detectable by XRD, indicating that even if produced, PtS particles were too small.

High-resolution electron microscopy showed the presence of thin flat particles on the zirconia surface with lattice distances corresponding to that of PtS. They were probably produced, after the initial surface interaction of $H_2S$ with Pt, reorganizing it gradually into a PtS lattice. We attributed the appearance of flat Pt and PtS in the same particle to this interaction. No "PtS overlayer" could be observed over metallic Pt particles. The loss of catalytic activity, however, points to poisoning of the residual Pt surface, likely by dispersed surface sulfur entities. The thinness of PtS particles could facilitate their reduction to metallic Pt.

XPS showed no sulfide component after quasi in situ hydrogen treatment. This treatment reactivated the (smaller) ensembles for C=C double-bond hydrogenation but the three-atom arrays necessary for hydrogenating benzene remained inactive.

## Acknowledgments

The authors are grateful to Dr. Gábor Resofszki for synthesizing the original Pt/sulfated zirconia samples. Z.P. thanks the Hungarian National Science Foundation (OTKA T037241) for support. We thank one of the referees for inspiring the additional utilization of catalytic reactions for surface characterization.

## References

[1] B.H. Davis, R.A. Keogh, R. Srinivasan, Catal. Today 20 (1994) 219.
[2] X. Song, A. Sayari, Catal. Rev. Sci. Eng. 38 (1996) 329.
[3] K. Tanabe, H. Hattori, in: G. Ertl, H. Knözinger, J. Weitkamp (Eds.), Handbook of Heterogeneous Catalysis, vol. 1, Chemie, Weinheim, 1997, p. 404.
[4] S. Rezgui, R.E. Jentoft, B.C. Gates, Catal. Lett. 51 (1998) 229.
[5] J.C. Yori, J.C. Luy, J.M. Parera, Appl. Catal. 46 (1989) 103.
[6] F. Garin, D. Andriamasinoro, A. Abdulsamad, J. Sommer, J. Catal. 131 (1991) 199.
[7] S.Y. Kim, J.G. Goodwin, S. Hammache, A. Auroux, D. Galloway, J. Catal. 201 (2001) 1.
[8] R.A. Comelli, R. Finelli, S.R. Vaudagna, N.S. Figoli, Catal. Lett. 45 (1997) 227.
[9] E. Iglesia, S.L. Soled, G.M. Kramer, J. Catal. 144 (1993) 238.
[10] J.C. Duchet, D. Gulliaume, A. Monnier, C. Dujardin, J.P. Gilson, J. van Gestel, A. Szabo, P. Nascimento, J. Catal. 198 (2001) 328.
[11] K. Ebitani, H. Konno, T. Tanaka, H. Hattori, J. Catal. 135 (1992) 60.
[12] T. Shishido, T. Tanaka, H. Hattori, J. Catal. 172 (1997) 24.
[13] Z. Paál, M. Muhler, R. Schlögl, J. Catal. 143 (1993) 318.
[14] K. Ebitani, H. Konno, T. Tanaka, H. Hattori, J. Catal. 143 (1993) 322.
[15] T. Tanaka, T. Shishido, H. Hattori, K. Ebitani, S. Yoshida, Physica B 208/209 (1995) 649.
[16] A. Sayari, A.J. Dicko, J. Catal. 145 (1994) 561.
[17] J. Zhao, G.P. Huffman, B.H. Davis, Catal. Lett. 24 (1994) 385.
[18] H. Liu, H. Lei, W.M.H. Sachtler, Appl. Catal. A 137 (1996) 167.
[19] J.M. Grau, C.R. Vera, J.M. Parera, Appl. Catal. A 227 (2002) 217.
[20] A. Ghenciu, D. Farcasiu, Catal. Lett. 44 (1997) 30.
[21] T. Buchholz, U. Wild, M. Muhler, G. Resofszki, Z. Paál, Appl. Catal. A 189 (1999) 225.
[22] J.-M. Manoli, C. Potvin, M. Muhler, U. Wild, G. Resofszki, T. Buchholz, Z. Paál, J. Catal. 178 (1998) 338.
[23] Z. Paál, U. Wild, M. Muhler, J.-M. Manoli, C. Potvin, T. Buchholz, S. Sprenger, G. Resofszki, Appl. Catal. A 188 (1999) 257.
[24] Z. Paál, M. Muhler, K. Matusek, Appl. Catal. A 149 (1997) 113.
[25] Z. Paál, M. Muhler, K. Matusek, J. Catal. 175 (1998) 245.
[26] Z. Paál, P. Tétényi, M. Muhler, J.-M. Manoli, C. Potvin, J. Chem. Soc. Faraday Trans. 94 (1998) 459.
[27] D.J. Smith, D. White, T. Baird, J.R. Fryer, J. Catal. 81 (1983) 107.
[28] J.-R. Chang, S.-L. Chang, T.-B. Lin, J. Catal. 169 (1997) 338.
[29] J. van Gestel, V.T. Nghiem, D. Guillaume, J.P. Gilson, J.C. Duchet, J. Catal. 212 (2002) 173.
[30] S. Roberts, R.J. Gorte, J. Chem. Phys. 93 (1990) 5337.
[31] C. Morterra, G. Cerrato, S. Di Cerio, M. Signoretto, F. Pinna, G. Strukul, J. Catal. 165 (1997) 172.
[32] C.R. Vera, J.C. Yori, C.L. Pieck, S. Irusta, J.M. Parera, Appl. Catal. A 240 (2003) 161.
[33] Z. Paál, R. Schlögl, Surf. Interface Anal. 19 (1992) 524.
[34] D.R. Milburn, R.A. Keogh, R. Srinivasan, B.H. Davis, Appl. Catal. A 147 (1996) 109.
[35] C. Morant, J.M. Sanz, L. Galán, L. Soriano, F. Rueda, Surf. Sci. 218 (1989) 331.

[36] A. Katrib, J. Electron Spectrosc, Relat. Phenom. 18 (1980) 275.
[37] K.S. Kim, N. Winograd, R.E. Davis, J. Am. Chem. Soc. 93 (1971) 6296.
[38] J. Dembowski, L. Marosi, M. Essig, Surf. Sci. Spectra 2 (1994) 104.
[39] M. Muhler, Z. Paál, Surf. Sci. Spectra 4 (1997) 125.
[40] E. Fülöp, V. Gnutzmann, Z. Paál, W. Vogel, W., Appl. Catal. 66 (1990) 319.
[41] J.V. Niemantsverdriet, Spectroscopy in Catalysis, VCH, Weinheim, 1993.
[42] J.T. Miller, B.C. Meyers, F.S. Modica, G.S. Lane, M. Vaarkamp, D.C. Koningsberger, J. Catal. 143 (1993) 395.
[43] A. Iordan, M.I. Zaki, C. Kappenstein, J. Chem. Soc. Faraday Trans. 89 (1993) 2527.
[44] J.N. Beltramini, in: G.J. Antos, A.M. Aitani, J.M. Parera (Eds.), Catalytic Naphtha Reforming, Dekker, New York, 1995, p. 365.
[45] B.A. Horrell, D.L. Cocke, Catal. Rev. Sci. Eng. 29 (1987) 447.
[46] D. Spielbauer, G.A.H. Mekhemer, M.I. Zaki, H. Knözinger, Catal. Lett. 40 (1996) 71.
[47] C.R. Vera, C.L. Pieck, K. Shimizu, J.M. Parera, Appl. Catal. A 230 (2002) 137.
[48] W. Hua, J. Sommer, Appl. Catal. A 227 (2002) 279.
[49] F.R. Chen, G. Coudurier, J.-F. Joly, J.C. Vedrine, J. Catal. 143 (1993) 616.
[50] E. Taglauer, H. Knözinger, Phys. Stat. Sol. B 192 (1995) 465.
[51] F.J. Gracia, J.T. Miller, A.J. Kropf, E.E. Wolf, J. Catal. 209 (2002) 341.
[52] (a) E. Ruckenstein, I. Sushumna, in: Z. Paál, P.G. Menon (Eds.), Hydrogen Effects in Catalysis, Dekker, New York, 1988, p. 259;
(b) I. Sushumna, E. Ruckenstein, J. Catal. 108 (1987) 77.
[53] P. Biloen, J.N. Helle, H. Verbeek, F.M. Dautzenberg, W.M.H. Sachtler, J. Catal. 63 (1980) 112.
[54] G. Rupprechter, G.A. Somorjai, J. Phys. Chem. B 103 (1999) 1623.
[55] A. Wootsch, L. Pirault-Roy, J. Leverd, M. Guérin, Z. Paál, J. Catal. 208 (2002) 490.
[56] D. Spielbauer, G.A.H. Mekhemer, E. Bosch, H. Knözinger, Catal. Lett. 36 (1996) 59.